Geophys. J. Int. (1993) **113**, 524–534

RESEARCH NOTE

Strike-angle determination from the magnetotelluric impedance tensor in the presence of noise and local distortion: rotate at your peril!

Alan G. Jones[1] and Ross W. Groom[2]

[1] *Geological Survey of Canada, 1 Observatory Crescent, Ottawa, Ontario, K1A 0Y3, Canada*
[2] *Department of Geological Sciences, Queen's University, Kingston, Ontario, K7L 3N6, Canada*

Accepted 1992 October 7. Received 1992 September 29; in original form 1992 June 5

SUMMARY

Determination of the strike of the dominant 2-D geoelectrical structure from magnetotelluric (MT) data is difficult in the presence of both noise and local distortion. This paper illustrates that often the strike angle is the least-stable parameter that can be resolved from the MT data themselves, and that the telluric distortion parameters are usually more robustly estimated. In particular, techniques which rely only on the analytical rotational properties of the MT impedance tensor can yield erroneous results in the presence of even small amounts of noise. The estimation procedure is stabilized once the telluric distortion parameters have been correctly determined and a constrained fit is sought. Also, it is emphasized that even when the true strike angle is known, statistically superior estimates of the regional impedances result when fitting a galvanic distortion model to the data rather than merely rotating the impedance tensor into the determined (or assumed) strike direction.

Key words: magnetotelluric data analysis, magnetotelluric tensor decomposition.

INTRODUCTION

One of the most important decisions made when interpreting magnetotelluric (MT) data is that of the strike angle for the interpretation coordinate frame. This coordinate frame imposes a structure on the data which may lead to erroneous models if chosen incorrectly. Typically, the interpreter uses other information, such as geological trends, as well as that offered by the MT data when choosing the strike angle. However, in such cases it is incumbent upon the interpreter to show that the MT data themselves support the choice of strike angle.

The intent of this note is to illustrate that strike determination from MT data is unstable in the presence of local distortion and even small amounts of noise, and that rotation of the impedance tensor to fit some 2-D analytical form is particularly questionable. In addition, it is shown that once having determined the correct strike angle, statistically superior estimates of the regional 2-D impedances result from fitting a galvanic distortion model to the data rather than merely rotating the impedance tensor to the adopted strike direction.

We assume from the outset that a model of 3-D surficial distortion overlying a 2-D regional conductivity structure is valid. Tests for the validity of such a model can be found in Groom & Bailey (1989, 1991), Groom & Bahr (1992) and Bahr (1991).

THEORY

The MT impedance tensor relates the horizontal electric and magnetic field components by a 2×2 complex transfer function, viz:

$$\boldsymbol{E} = \begin{pmatrix} E_x \\ E_y \end{pmatrix} = \boldsymbol{Z}\boldsymbol{H} = \begin{pmatrix} Z_{xx} & Z_{xy} \\ Z_{yx} & Z_{yy} \end{pmatrix} \begin{pmatrix} H_x \\ H_y \end{pmatrix} \tag{1}$$

(dependence on frequency assumed), where $\boldsymbol{E}$, $\boldsymbol{H}$ and $\boldsymbol{Z}$ are in S.I. units ($\mathrm{V\,m^{-1}}$, $\mathrm{A\,m^{-1}}$ and Ω respectively).

In order to make modelling of multidimensional MT data more tractable, it has become common to express distortions of the electric (telluric) field caused by local, near-surface inhomogeneities by a 2×2 matrix of real, frequency-independent numbers, $\mathbf{C}$. This scattering matrix operates on

the regional MT impedance tensor $\mathbf{Z}_r$, to give the observed MT independance tensor, $\mathbf{Z}_o$,

$$\mathbf{Z}_o = \mathbf{C}\mathbf{Z}_r \tag{2}$$

where

$$\mathbf{C} = \begin{pmatrix} c_{xx} & c_{xy} \\ c_{yx} & c_{yy} \end{pmatrix} \tag{3}$$

(see review by Groom & Bahr 1992, and references therein). The most general case is when $\mathbf{Z}_r$ describes induction in 3-D conductivity structures. This is termed '3-D over 3-D' (3-D/3-D) and usually cannot be addressed with the MT interpretative tools currently available. However, a more restrictive, but often valid, case is now being used for the interpretation of much MT data in which the regional response is modelled as 2-D with distortion by 3-D surficial scattering (3-D/2-D). For this model, the MT observations in an arbitrary coordinate frame are related to the 2-D regional response by

$$\mathbf{Z}_o(\theta) = \mathbf{R}(\theta)\mathbf{C}\mathbf{Z}_{2\text{-D}}\mathbf{R}^{\mathrm{T}}(\theta), \tag{4}$$

where $\mathbf{R}$ is a rotation matrix, T denotes transpose, and $\mathbf{Z}_{2\text{-D}}$, the regional 2-D MT impedance tensor, is given by

$$\mathbf{Z}_{2\text{-D}} = \begin{pmatrix} 0 & Z_{xy} \\ Z_{yx} & 0 \end{pmatrix} \tag{5}$$

(Bahr 1988, 1991; Groom & Bailey 1989, 1991; Chakridi, Chouteau & Mareschal 1992).

Bahr (1988) proposed a method for determining the appropriate strike angle based on the analytical rotational properties of $\mathbf{Z}_o$. He showed that when the observed noise-free tensor is rotated into the correct strike coordinate frame, the phases of the two elements in each column of the rotated impedance tensor are equal, i.e.

$$\mathbf{Z}_o(0) = \mathbf{C}\mathbf{Z}_{2\text{-D}} = \begin{pmatrix} c_{xy}Z_{yx} & c_{xx}Z_{xy} \\ c_{yy}Z_{yx} & c_{yx}Z_{xy} \end{pmatrix} \tag{6}$$

(where 0 denotes that the observed impedance tensor is in the correct strike coordinate frame). Obviously, when two complex numbers have the same phase their ratio is totally real. Defining the phases of the complex ratios of the observed impedance tensor column elements by

$$\psi_1(\theta) = \tan^{-1}\left\{\frac{\mathrm{Imag}[Z_{xx_o}(\theta)/Z_{yx_o}(\theta)]}{\mathrm{Real}[Z_{xx_o}(\theta)/Z_{yx_o}(\theta)]}\right\} \tag{7}$$

and

$$\psi_2(\theta) = \tan^{-1}\left\{\frac{\mathrm{Imag}[Z_{xy_o}(\theta)/Z_{yy_o}(\theta)]}{\mathrm{Real}[Z_{xy_o}(\theta)/Z_{yy_o}(\theta)]}\right\}, \tag{8}$$

Bahr (1988, eq. 11) suggested that two angles be calculated which will fulfil the conditions that $\psi_1 = 0$ or π and simultaneously $\psi_2 = 0$ or π. The analytical formulae for derivation of the strike angles are functions of sums and differences of the diagonal and off-diagonal elements of the impedance tensor. Alternatively, the interpreter could rotate the observed impedance tensor and seek numerically the appropriate strike angle. This approach has been used by Zhang, Roberts & Pedersen (1987), Bahr (1988, 1991) and Chakridi *et al.* (1992) to define MT strike. Note that in the case of either no distortion, or symmetric distortion which takes the form $c_{xy} = c_{yx} = 0$, angles ψ_1 and ψ_2 are undefined along the strike axes, and asymptotically approach

$$\psi_1(0) = \tan^{-1}\left\{\frac{\mathrm{Imag}[(c_{xx}Z_{xy} + c_{yy}Z_{yx})/c_{yy}Z_{yx}]}{\mathrm{Real}[(c_{xx}Z_{xy} + c_{yy}Z_{yx})/c_{yy}Z_{yx}]}\right\}$$

and

$$\psi_2(0) = \tan^{-1}\left\{\frac{\mathrm{Imag}[c_{xx}Z_{xy}/-(c_{xx}Z_{xy} + c_{yy}Z_{yx})]}{\mathrm{Real}[c_{xx}Z_{xy}/-(c_{xx}Z_{xy} + c_{yy}Z_{yx})]}\right\}$$

as the strike direction is approached. This difficulty was recognized by Bahr (1988) who gave a simpler formula, equivalent to Swift's (1967) strike formula, for use in determining the strike in this noise- and distortion-free case.

Alternatively, one could appeal to other rotational properties of $\mathbf{Z}$ and estimate not the strike angle itself, but the angle which is 45° from strike. At this angle, the rotated impedance tensor assumes the form

$$\begin{aligned}\mathbf{Z}_o(45) &= \begin{bmatrix} Z_{xx}(45) & Z_{xy}(45) \\ Z_{yx}(45) & Z_{yy}(45) \end{bmatrix} \\ &= \frac{1}{2}\begin{bmatrix} 1 & 1 \\ -1 & 1 \end{bmatrix}\begin{bmatrix} c_{xx} & c_{xy} \\ c_{yx} & c_{yy} \end{bmatrix}\begin{bmatrix} 0 & Z_{xy} \\ Z_{yx} & 0 \end{bmatrix}\begin{bmatrix} 1 & -1 \\ 1 & 1 \end{bmatrix} \\ &= \frac{1}{2}\begin{bmatrix} (c_{xx} + c_{yx})Z_{xy} + (c_{xy} + c_{yy})Z_{yx} \\ (c_{xx} + c_{yx})Z_{xy} - (c_{xy} + c_{yy})Z_{yx} \\ (c_{yx} - c_{xx})Z_{xy} + (c_{yy} - c_{xy})Z_{yx} \\ (c_{yx} - c_{xx})Z_{xy} - (c_{yy} - c_{xy})Z_{yx} \end{bmatrix}.\end{aligned} \tag{9}$$

Thus

$$\begin{aligned} Z_{xx}(45) + Z_{xy}(45) &= (c_{xx} + c_{yx})Z_{xy} \\ Z_{xx}(45) - Z_{xy}(45) &= (c_{xy} + c_{yy})Z_{yx} \\ Z_{yx}(45) + Z_{yy}(45) &= (c_{yx} - c_{xx})Z_{xy} \\ Z_{yx}(45) - Z_{yy}(45) &= (c_{yy} - c_{xy})Z_{yx} \end{aligned}$$

and two phases can be formed from the complex ratios of the sums and differences of the observed row elements which serve as estimators for this direction,

$$\psi_3(\theta) = \tan^{-1}\left\{\frac{\mathrm{Imag}[(Z_{xx}(\theta) + Z_{xy}(\theta))/(Z_{yx}(\theta) + Z_{yy}(\theta))]}{\mathrm{Real}[(Z_{xx}(\theta) + Z_{xy}(\theta))/(Z_{yx}(\theta) + Z_{yy}(\theta))]}\right\} \tag{10}$$

$$\psi_4(\theta) = \tan^{-1}\left\{\frac{\mathrm{Imag}[(Z_{xx}(\theta) - Z_{xy}(\theta))/(Z_{yx}(\theta) - Z_{yy}(\theta))]}{\mathrm{Real}[(Z_{xx}(\theta) - Z_{xy}(\theta))/(Z_{yx}(\theta) - Z_{yy}(\theta))]}\right\} \tag{11}$$

for which $\psi_3 = 0$ or π and simultaneously $\psi_4 = 0$ or π when the correct angle 45° from strike is found. These estimators, ψ_3 and ψ_4, have the appeal that they do not suffer from inherent instability when there is no distortion (or only anisotropy distortion), but asymptote to 0° or π at 45° from strike.

In contrast to empirical rotation of the MT tensor to find a 2-D analytical form, Groom & Bailey (1989, 1991) proposed a tensor decomposition method (referred to hereafter as the GB method) which fits a 3-D/2-D distortion model to the observed impedances. The scattering tensor $\boldsymbol{C}$ is factored as a product of modified forms of the Pauli spin matrices multiplied by a scalar site gain, viz.

$$\boldsymbol{C} = g\boldsymbol{TSA} = g\begin{pmatrix} 1 & -t \\ t & 1 \end{pmatrix}\begin{pmatrix} 1 & e \\ e & 1 \end{pmatrix}\begin{pmatrix} 1+s & 0 \\ 0 & 1-s \end{pmatrix} \tag{12}$$

where g is the *site gain*, $\boldsymbol{T}$ is a 'twist' tensor, $\boldsymbol{S}$ describes a 'shear' tensor, and $\boldsymbol{A}$ is an anisotropy tensor. From the MT data alone, g cannot be determined, and s is evaluated by requiring the high-frequency asymptotes in the two modes to be equal. The remaining seven unknowns, which are the remaining two descriptors of telluric distortion (twist, t, and shear, e), the regional strike angle (θ), and the two complex regional impedances (Z_{xy} and Z_{yx}), are determined by statistically fitting the eight data to these seven parameters (see Groom *et al.* 1992, for details). Over a band of N frequencies, the method is to find the simplest distortion model possible, which occurs when *twist, shear* and the regional strike are frequency independent. In this case, the number of degrees of freedom is reduced from $7N$ to $4N+3$. The shear and twist values are commonly presented as angles, determined by taking the arctangents of t and e. Whilst the telluric distortion parameters, characterized herein as twist and shear, have little intrinsic merit, it will be shown that their determination stabilizes the estimation of strike.

THEORETICAL EXAMPLE

To illustrate the lack of sensitivity in the MT impedance tensor to the strike angle, we choose the theoretical response from a 2-D model of the North American Central Plains (NACP) conductivity anomaly (Jones & Craven 1990).

The model responses at the period (100 s) of greatest induction in the anomaly, at which there is the largest separation between the E- and B-polarization phase responses, are

$$\boldsymbol{Z}_{2\text{-D}}(0) = \begin{bmatrix} 0 & (4.72, 4.05) \\ (-8.25, -3.10) & 0 \end{bmatrix} \times 10^{-4} (\Omega), \qquad (13)$$

i.e. $\rho_{xy} = 4.89\ \Omega \cdot m$, $\phi_{xy} = 40.6°$, $\rho_{yx} = 9.82\ \Omega \cdot m$, and $\phi_{xy} = -159.4°$, where the xy element denotes the E-polarization responses, and yx denotes B-polarization responses.

An example impedance tensor, which is distorted but free of noise, can be derived using the distortion tensor, $\boldsymbol{C}$, of

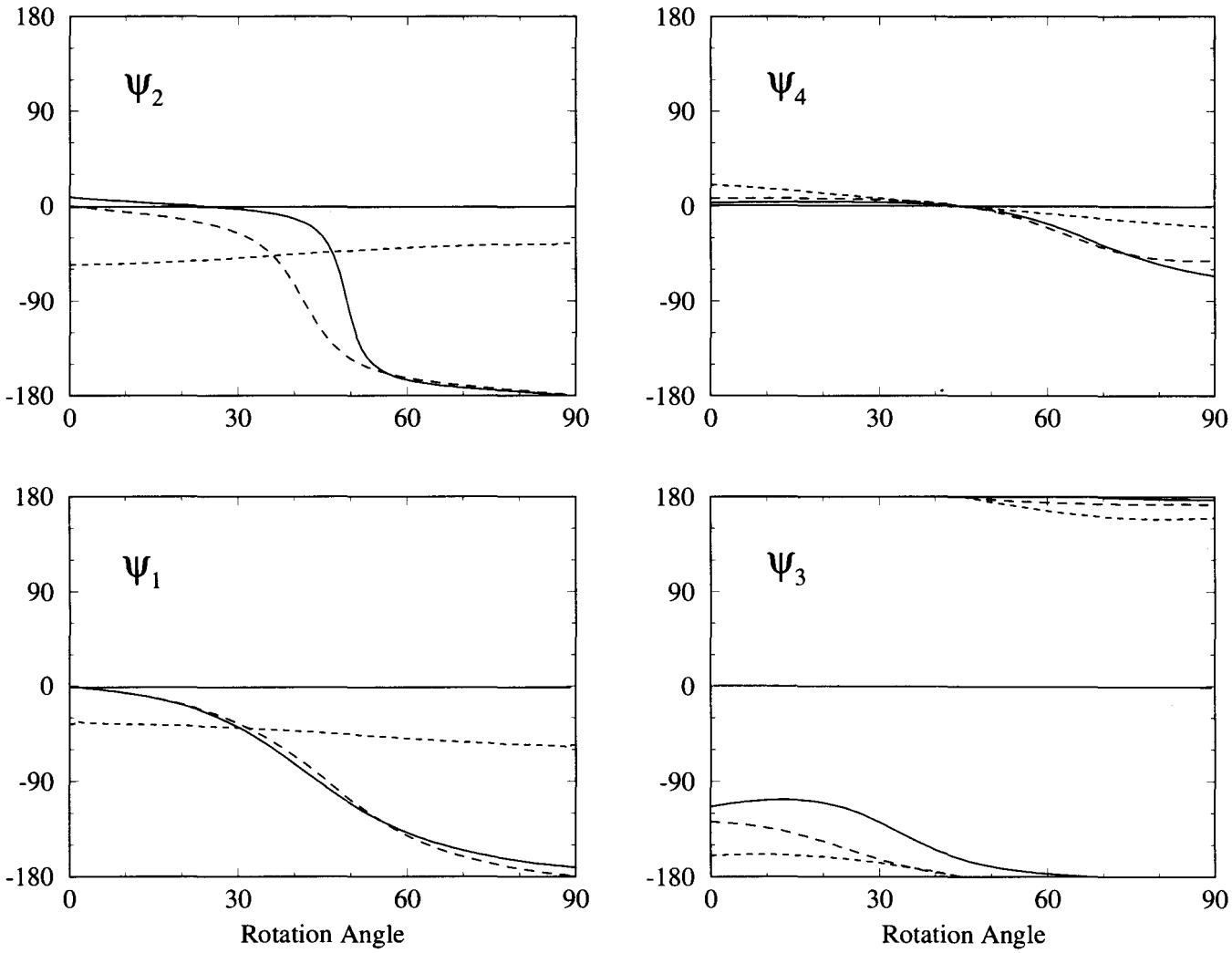

Figure 1. Variation of the four angles, ψ_1, ψ_2, ψ_3 and ψ_4, as tensors (13), (14) and (15) are rotated through 0°–90°. The *short dashed curves* are for tensor (13) which represents a noise and distortion free case. Note that ψ_1 and ψ_2 do not cross 0° or 180° and so do not conform to the model. The *long dashed curves* are for tensor (14) which represents a distorted but noise-free case. All four estimators yield the correct result for the strike direction. The *solid curves* are for tensor (15) which represents noisy distorted data. Estimators ψ_1 and ψ_4 perform well for this particular noise realization.

Chakridi *et al.* (1992) (this tensor corresponds to distortion at a site located close to the embedded hemisphere of Groom & Bailey 1991). We obtain

$$\boldsymbol{Z}(0) = \begin{pmatrix} 1.26 & 0.44 \\ 0.53 & 0.86 \end{pmatrix} \boldsymbol{Z}_{2\text{-D}}$$

$$= \begin{bmatrix} (-3.63, -1.36) & (5.95, 5.10) \\ (-7.10, -2.67) & (2.51, 2.15) \end{bmatrix} \times 10^{-4}(\Omega). \qquad (14)$$

Decomposition of the distortion tensor above in terms of the GB parameters yields a site gain (g) of 1.06, an anisotropy (s) of 0.172, a twist angle of $-2.1°$ (i.e. $t = -0.037$), and a shear angle of 24.95° (i.e. $e = 0.47$). (Note that in general with field data it is impossible to determine the site gain without other information; this is the well known MT static shift, e.g. Jones 1988.) In this unrotated coordinate frame, the phases of both elements of column 1 are $-159.4°$, and of both elements of column 2 are 40.6°, showing that the tensor fits the model of eq. (6).

From this tensor we generate noise-contaminated statistical realizations by adding a reasonable amount of Gaussian noise to these values (standard deviation of ≈4.5 per cent of the magnitude of the largest element). One of these realizations is

$$\boldsymbol{Z}(0) = \begin{bmatrix} (-3.42, -1.15) & (6.19, 5.00) \\ (-7.69, -2.62) & (3.28, 3.57) \end{bmatrix} \times 10^{-4}(\Omega). \qquad (15)$$

Rotating the three tensors, (13), (14) and (15), through 0°–90° and determining the four strike estimators $\psi_1, \psi_2, \psi_3, \psi_4$, gives the three curves on each of the four plots of Fig. 1. In the absence of distortion (*short dashed* curves on Fig. 1), estimators ψ_3 and ψ_4 behave well and give the correct strike direction; ψ_1 and ψ_2 are undefined at the correct strike angle of 0° (and 90°). For the distorted but noise-free tensor (*long dashed* curves), all four estimators give the correct strike direction, but it should be noted that ψ_3 and ψ_4 have a larger gradient in the region of 0° than do ψ_1 and ψ_2, and thus are intrinsically more sensitive to the strike angle. For the noisy and distorted realization of eq. 15, by chance two of the estimators (ψ_1 and ψ_4) perform well, but the other two perform poorly. Bahr's (1988, eq. 11) analytical formulae give 0.4° and 67.5° for ψ_1 and ψ_2 respectively, which concurs with our observation that ψ_1 performs well. Bahr's modified 'robust' formulae (Bahr 1991, eq. 30) yield strike angles of 19.0° and 109.0°, which are now correctly 90° apart but in error by nineteen degrees.

Deriving twenty statistical realizations of noise-contaminated distorted tensors illustrates that these four estimators generally perform poorly (Fig. 2). In particular, ψ_1 and ψ_2 did not give an estimate, i.e. did not cross 0° or π, in three to four of the twenty realizations. The ranges of angles from the estimators were: $\psi_1 = -18°$ to 23° (from 17 of 20), $\psi_2 = -18°$ to 19° (from 16 of 20), $\psi_3 = 28°$ to 64°

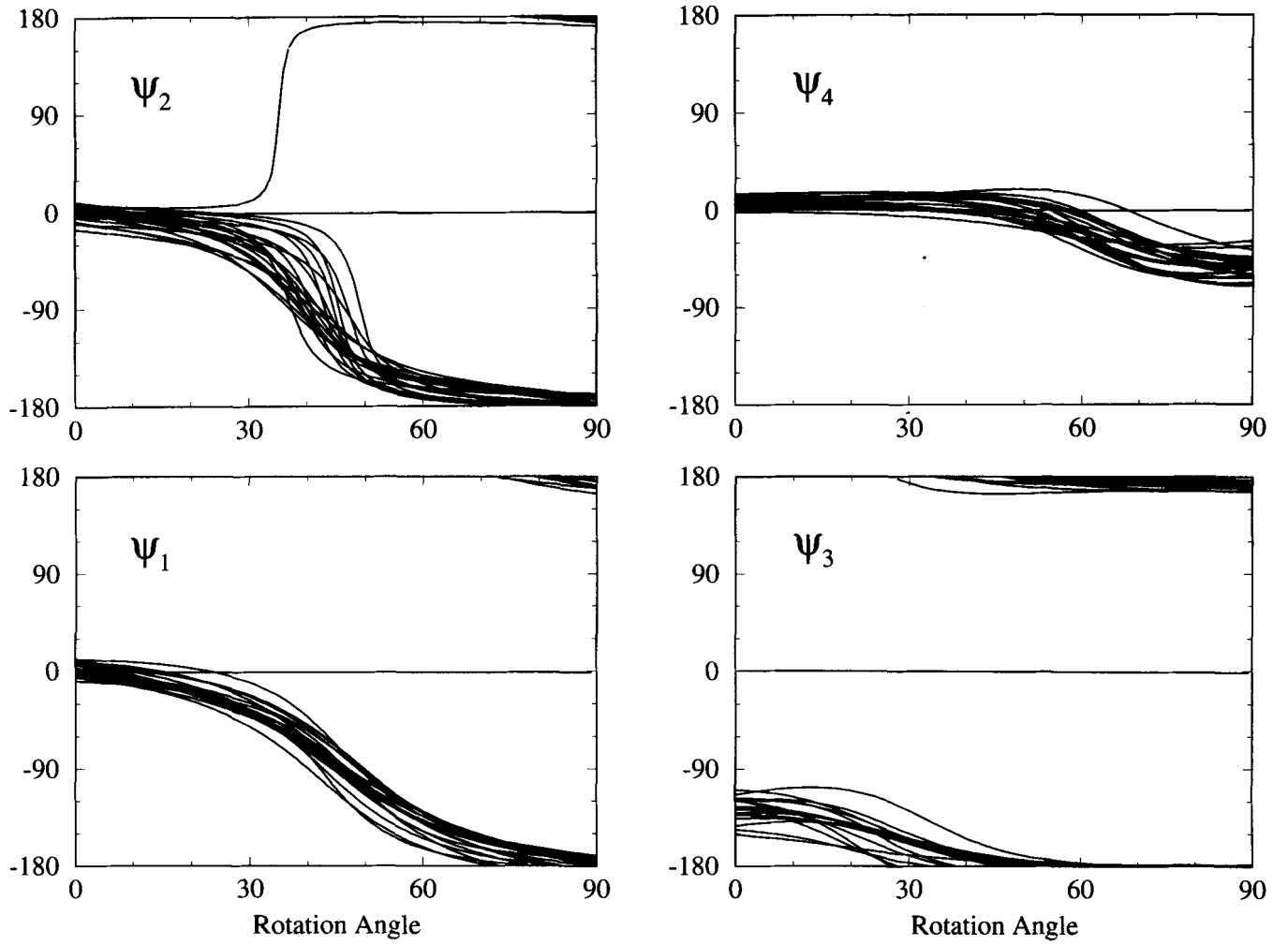

Figure 2. Variation of the four angles, ψ_1, ψ_2, ψ_3 and ψ_4, as twenty noise-contaminated realizations of tensor (14) are rotated through 0°–90°.

(equivalent to $-17°$ to $19°$), and $\psi_4 = 32°$ to $68°$ (equivalent to $-13°$ to $23°$) (from all 20 in both cases). The two estimators ψ_3 and ψ_4 thus proved more robust and led to superior estimates of the strike angle than did ψ_1 and ψ_2.

GB decomposition of tensor (15) yielded a *twist* distortion of $0° \pm 1.5°$, $27° \pm 1°$ for the *shear* angle, and a strike angle of $8° \pm 4°$. The shear angle is determined correctly, the twist is determined to better than one and one-half standard errors, whereas the rotation direction is determined to within two standard errors. In addition, the phases were reasonably well recovered, with $\phi_{xy} = 39.1°$ and $\phi_{yx} = -164.4°$, compared to $40.6°$ and $-159.4°$ respectively for the undistorted data.

Figs 3 and 4 show GB analyses of thirty-one noise-contaminated realizations of tensor (14) with noise added. Twist and shear scatter around the correct values of just less than $0°$ and $25°$ respectively. Fig. 4 displays the histograms of strike, twist and shear from the thirty-one realizations, and the stability of the estimate of shear, compared to the other two, is clearly seen. We have found that the telluric distortion parameters, characterized here as twist and shear, are usually more stable under decomposition than is the strike-angle determination (Groom *et al.* 1992). Holding the shear and twist parameters constant at their average values of $24.8°$ and $-1.8°$ (compared to the ture values of $24.9°$ and $-2.1°$) respectively, reduces the range in strike angle determined from $34°$ to $24°$ with the median value around $-7° \pm 4°$. Note that this theoretical study illustrates that there can be inherent biases associated with the determination of the strike direction (see Groom *et al.* 1992) from noise contributions to the non-linear system.

In the absence of noise contributions the regional impedances derived by rotating into the strike coordinate system will be exactly the same as those determined by fitting a decomposition model to the data. However, it is important to recognize that, due to the bias effects of the noise contributions, rotating the data is *not* equivalent to fitting a decomposition model to the data. The two phase angles, ϕ_{xy} and ϕ_{yx}, derived from one thousand realizations by (1) rotating the data into the determined 'best' strike direction ($-7°$), and by (2) fitting a 3-D/2-D distortion model to the data with the determined distortion parameters (shear = $24.8°$, twist = $-1.8°$, strike = $-7°$), are illustrated in Fig. 5 (left and right columns respectively). Fitting a distortion model to the data yields improved estimates of the regional phases; they exhibit a smaller range, smaller variance (by 20–25 per cent), and more peaked distributions than the 2-D rotation estimates (see Table 1).

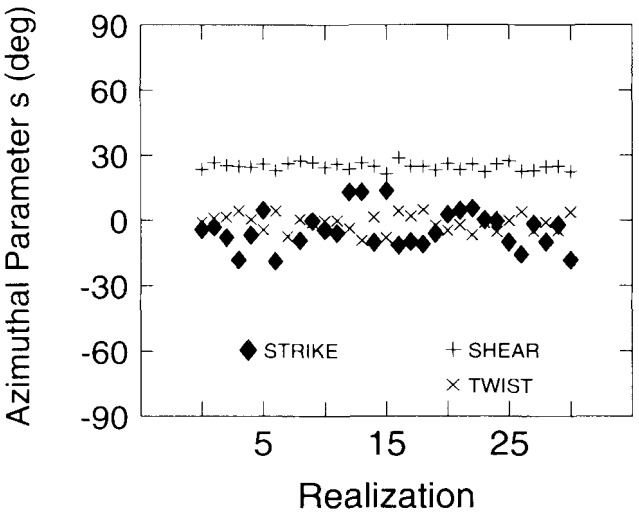

Figure 3. Groom–Bailey decomposition results from thirty-one (31) noise-contaminated realizations of tensor (14). × denotes the *twist* angle, + denotes the *shear* angle, and ◆ denotes the *strike* angle.

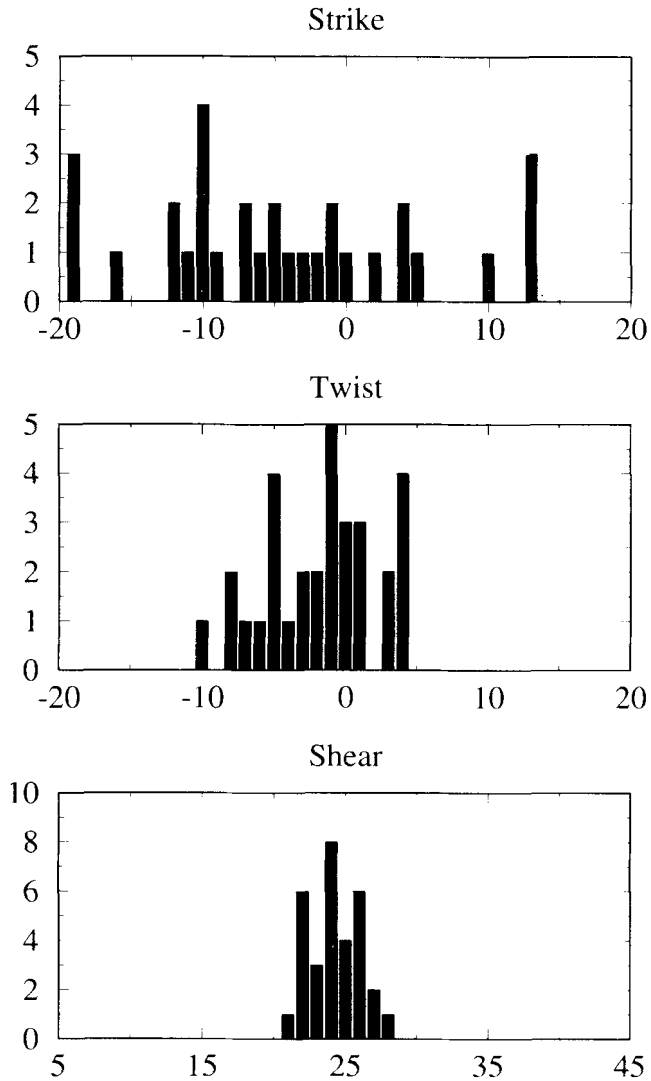

Figure 4. Histograms of the *strike*, *twist* and *shear* angles shown in Fig. 3. Note that the *shear* exhibits far less scatter, i.e. is more robustly determined, than either of the other two, and that the strike angle is the least robust parameter.

FIELD EXAMPLES

To illustrate the main points of this note with field data, MT responses from two sites located in southeastern British Columbia (Jones *et al.* 1988) are used. These two sites, named *lit007* and *lit008*, were recorded simultaneously as a ten-channel remote-reference pair. They were separated by ≈1 km, with site *lit008* at the bottom of the glacial Coffee Creek valley and *lit007* up the north side of the valley on a terrace. The data are shown in Fig. 6 for all four elements at

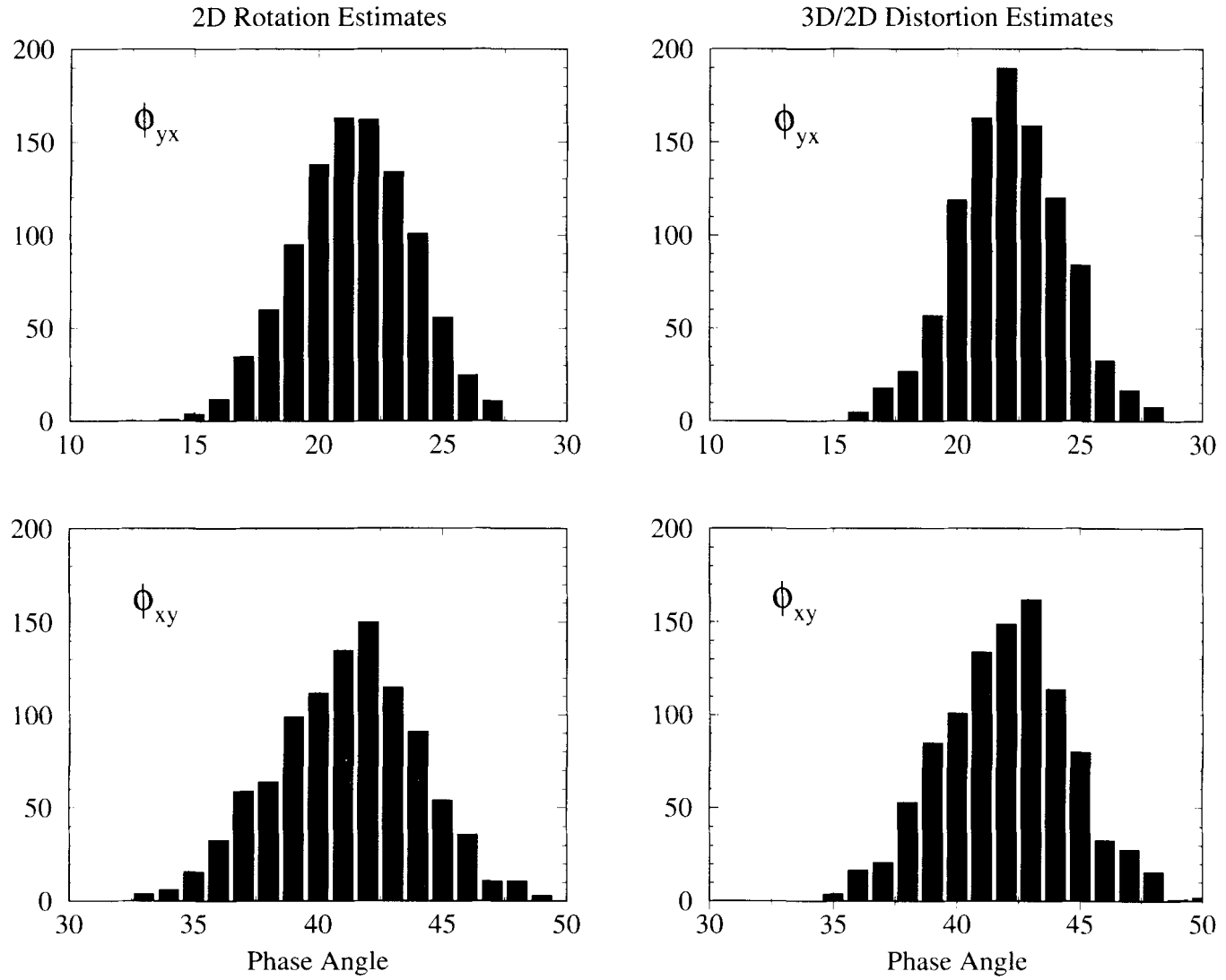

Figure 5. Histograms of estimates of ϕ_{xy} (lower row) and ϕ_{yx} (upper row) from one thousand noise-contaminated realizations. The left column are those estimates obtained by rotating the tensor into the determined strike direction (−7°), whereas the right column are those obtained by fitting a 3-D/2-D galvanic distortion model (shear = 24.8°, twist = −1.8°, strike = −7°).

Table 1. Statistics from 1000 estimates of ϕ_{xy} and ϕ_{yx} from (a) rotating the data into the determined coordinate frame (−7°), or (b) fitting the data to a 3-D/2-D distortion model with determined distortion parameters of shear = 24.8°, twist = −1.8° and strike = −7°.

	mean	variance	range
ϕ_{xy} 2D	41.6	8.3	16.9
ϕ_{yx} 2D	21.9	5.5	13.9
ϕ_{xy} 3D/2D	42.1	6.7	15.0
ϕ_{yx} 3D/2D	22.5	4.7	12.5

both sites in a geographic coordinate system. Although the phases from site *lit008* are well behaved, at site *lit007* the Z_{xy} and Z_{yy} phases, i.e. the second column of $\boldsymbol{Z}_7$, wrap around though 360° at periods greater than 1 s. Also note that for *lit007* the distortion is so severe that the smallest element over virtually the whole period range is one of the off-diagonal elements, Z_{xy}.

It is instructive to examine the inter-relationship between these two datasets. Fig. 7 shows the transfer function which gives *lit007* from *lit008*, i.e. $\boldsymbol{Z}_7 = \boldsymbol{T}\boldsymbol{Z}_8$, where $\boldsymbol{T}$ is a complex 2×2 tensor. At high frequencies, the elements of the transfer matrix $\mathbf{T}$ are all complex and vary with frequency. However, at periods in excess of ≈3 s, the imaginary parts of the elements asymptotically approach zero and the real parts become frequency independent (to within statistical errors).

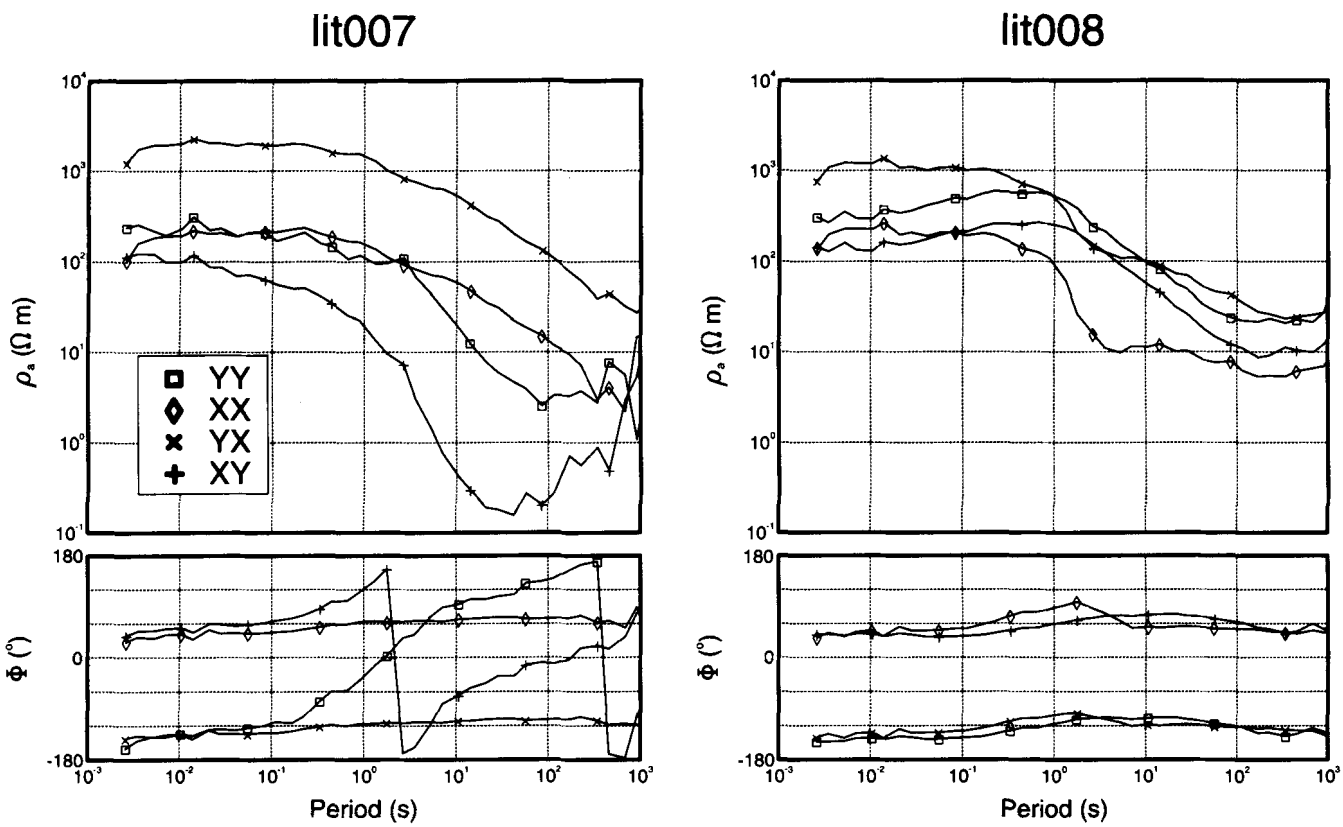

Figure 6. The MT data from sites *lit007* (left panel) and *lit008* (right panel).

At these long periods the two sites must be sensing the same regional geoelectrical structure(s), and so the difference between the two can be characterized as a static galvanic distortion given by

$$\boldsymbol{C} = \begin{pmatrix} -1.9 & -1.4 \\ 6.3 & 4.4 \end{pmatrix}. \tag{16}$$

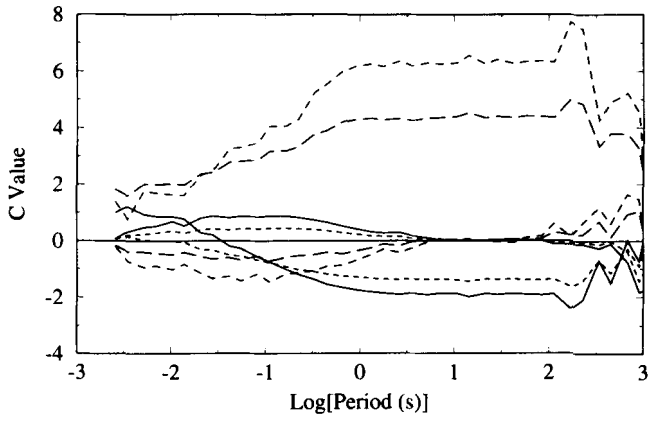

Figure 7. The elements of the complex 2×2 tensor which relates site *lit008* data to *lit007* data. The *solid* curves are for element c_{xx}, the short *dashed* curves are for element c_{xy}, the long *dashed* curves are for element c_{yx}, and the *dashed* curves are for element c_{yy} (bottom-to-top curves respectively at periods in the range 10–100 s). In the period range 3–100 s this tensor assumes the form of a galvanic distortion tensor $\boldsymbol{C}$ with zero imaginary parts and frequency-independent real parts. In this range, the four elements are: $c_{xx} = -1.9$, $c_{xy} = -1.4$, $c_{yx} = 6.3$ and $c_{yy} = 4.4$

This distortion tensor has the following GB parameters: $g = 1.86$, $s = 0.17$, $t = 1.90$ (62.2°), and $e = 0.985$ (44.5°); the high twist and shear indicate that the relative distortion between the two sites is extremely severe. Note that, however, the distortion tensor is only a relative one; the MT data from site *lit008* are obviously not true $\mathbf{Z}_{2\text{-D}}$ responses.

Groom & Bailey (1991) discuss an extension of the simple distortion model expressed by (2) to take into account the

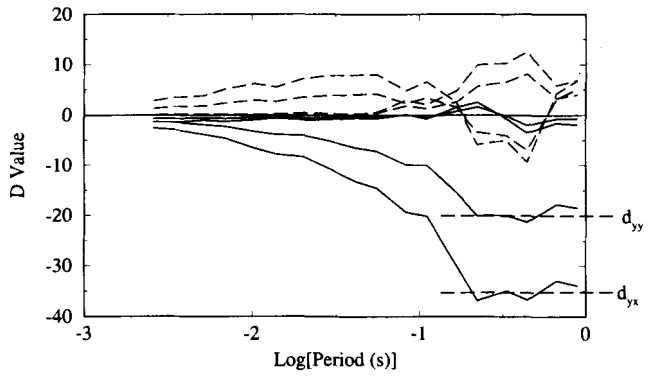

Figure 8. The elements of the complex 2×2 tensor which describes the effects of the magnetic fields of the galvanic charges. The *solid* curves are the real parts of each element, whereas the *dashed* curves are the imaginary parts. At periods in excess of 0.2 s the elements assume approximately the correct form of $\mathbf{D}$ with zero imaginary parts and frequency-independent real parts. In this range, there are only two elements that are significant, and are $d_{yx} = -34$ and $d_{yy} = -18$.

magnetic effect of the charges which occurs at high frequencies. This effect can be described by a 2×2 matrix of real, frequency-independent numbers, **D**, similar to **C** given in (3),

$$\mathbf{Z} = \mathbf{RC}[\mathbf{I} - \mathbf{Z}_{2\text{-}D}\mathbf{D}]\mathbf{Z}_{2\text{-}D}\mathbf{R}^{T}. \quad (17)$$

where **I** is the identity matrix. Note that the term $\mathbf{Z}_{2\text{-}D}\mathbf{D}$ decreases rapidly (compared to **I**) with increasing period, but is complex and so will primarily affect the phases of **Z**. Assuming the form of **C** given by (16) above, we can determine the elements of **D** which relate *lit007* to *lit008*. These are shown in Fig. 8 (real: *solid curves*, imaginary: *dashed*). Although there is noise due to the propagation of errors, **D** appears to adopt the correct form in the period range 0.2–1 s with close to zero imaginary parts and frequency independent real components. The two largest elements in the period range 0.2-1 s are d_{yx} and d_{yy} and these are ≈ -34 and ≈ -20 respectively.

Fig. 7 serves to illustrate that the data from sites *lit007* and *lit008* can be related to each other in terms of galvanic charge effects at periods in excess of 0.2 s, and that beyond 3 s the magnetic effects of these charges (Groom & Bailey 1991) become insignificant because of the decay of $\mathbf{Z}_{2\text{-}D}$ with increasing period. Accordingly, analyses of the data from these two sites at periods in the range 3–100 s should yield the same regional strike angle.

Figs 9 and 10 show the four ψ estimators for sites *lit007* and *lit008* respectively in the period range 3–100 s. It is clear from the two figures that a strike angle consistent over the period band and between the two sites cannot be chosen utilizing the rotational properties of $\mathbf{Z}_7$ and $\mathbf{Z}_8$.

Fig. 11 illustrates the GB unconstrained decomposition parameters for the two sites in the period range 1–100 s. The unconstrained decomposition models fit the data well, as indicated by the normalized χ^2-misfit statistic for each site (Groom *et al.* 1992). The data from site *lit007* indicate a strike angle of around $-60°$, whereas for site *lit008* the inversion yields a preference for $+120°$. Given the $\pi/2$ ambiguity, both of these sites therefore exhibit a consistent strike of either $+30°$ or $+120°$. Contour plots (not shown here) of the variation of the χ^2-misfit with rotation angle for both sites show strike angles in the range of around 30° give the lowest misfit errors. In Fig. 12 the strike angle at both sites has been constrained to fall within the range 25° to 35°. At the majority of periods, the strike angles found in these bounds are not one of the bounds themselves. The shear and

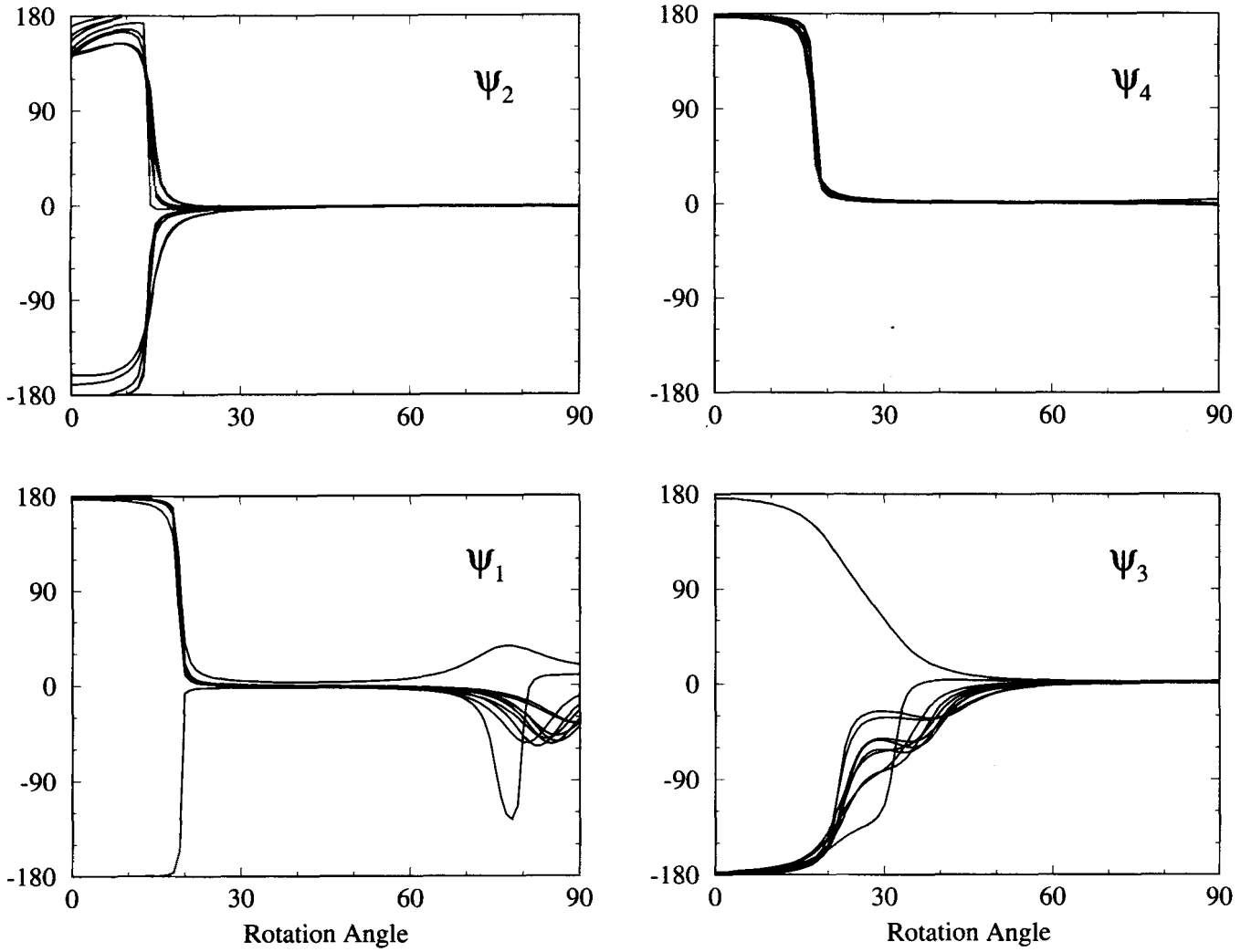

Figure 9. The variation of the four rotational estimators of the strike angle for the data from *lit007* in the period range 3–100 s. Each curve is for a different period in the band.

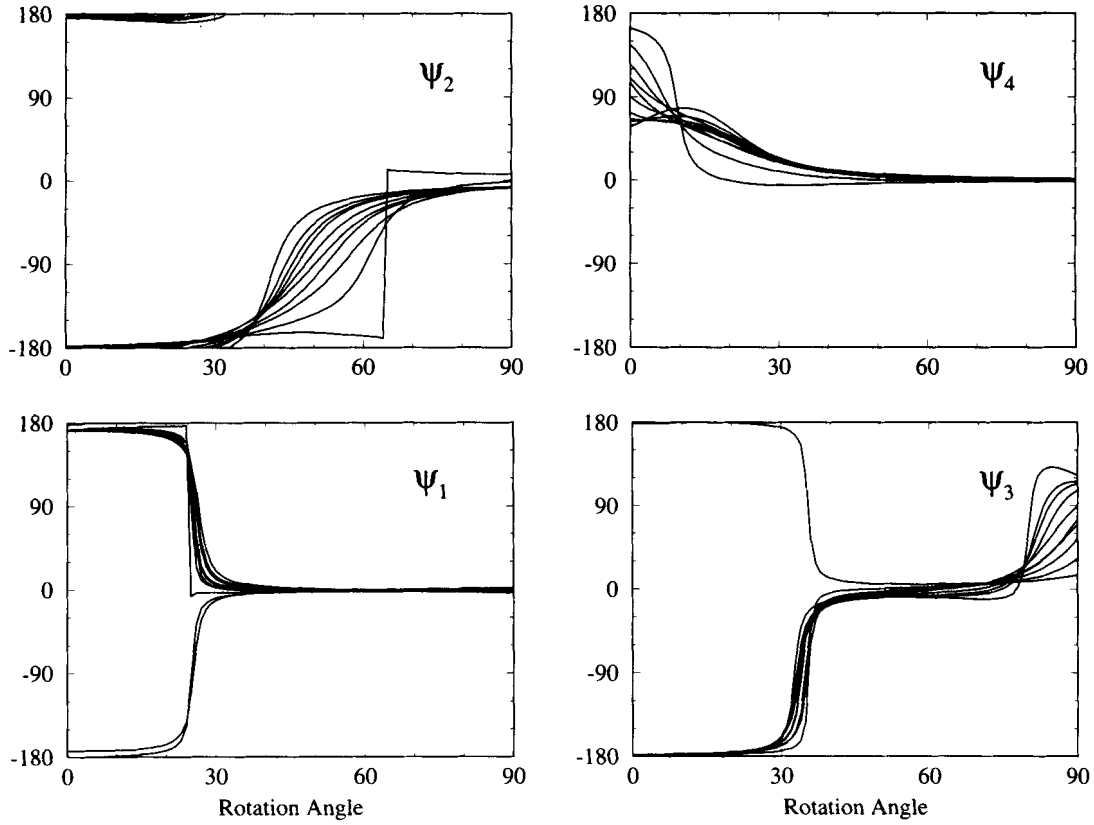

Figure 10. The variation of the four rotational estimators of the strike angle for the data from *lit008* in the period range 3–100 s Each curve is for a different period in the band.

twist exhibit virtually frequency-independent values (which are very different from the two sites), and the model fits to within acceptable errors. The recovered regional impedances in the strike directions of Fig. 12 are illustrated in Fig. 13, where the *xy* estimates are those with the electric field parallel to N30°E, and the *yx* estimates are with the electric field measured perpendicular to that direction, i.e. N60°W. The *yx* impedances from the two sites are particularly well recovered, and are within statistical accuracy at most periods. The *xy* estimates do not exhibit such consistency between the two sites, particularly at the shorter periods. This may be due to the galvanic-only distortion model being inappropriate at such short periods as shown by the imaginary components in Fig. 7.

CONCLUSIONS

The choice of the interpretation coordinate frame, i.e. of the appropriate strike angle, is of critical importance in MT studies. As such, although information from other sources, such as geological strike, can be used, it is incumbent upon the interpreter to show that the coordinate frame chosen is supported by the MT data.

We have demonstrated that determination of the regional strike angle from magnetotelluric data that are both contaminated by noise and distorted by local, near-surface, galvanic scatterers must be treated with care. In such circumstances, the parameters of the distorting structure, characterized here as twist and shear, are usually more stable over a period band than is the regional strike direction. In the field data chosen, by fitting a distortion model it is possible to extract a consistent strike direction from two sites 1 km apart which display severe distortion effects. It must be emphasized that one should be careful with the telluric distortion parameters; their choice imposes a coordinate system on the MT data which can lead to erroneous strike determination. We have found that the best approach with badly distorted data is to iterate between constraining the distortion parameters and the strike until a self-consistent result is obtained.

Given this instability in regional strike determination, one should not attempt to extract it by considering the rotational properties of the MT impedance tensor alone. If one does wish to study the rotational variation of $\mathbf{Z}$, then the parameters which define the angle 45° away from strike, ψ_3 and ψ_4 (eqs 10 and 11), are both more robust and more stable than ψ_1 and ψ_2. Although we advocate the use of statistics in order to determine both the telluric distortion parameters and to quantify the fit of the designated model to the dataset (Groom *et al.* 1992), an empirical rotation approach can be useful as a speedy aid in determining the type and extent of distortion present.

It is important to recognize that rotating the data into a given strike direction will yield statistically inferior regional responses to those obtained by fitting a 3-D/2-D distortion model to the data due to the noise contributions. Whilst the estimates of the major impedance (i.e. the larger of Z_{xy} or Z_{yx}) from the two schemes may be similar, the minor

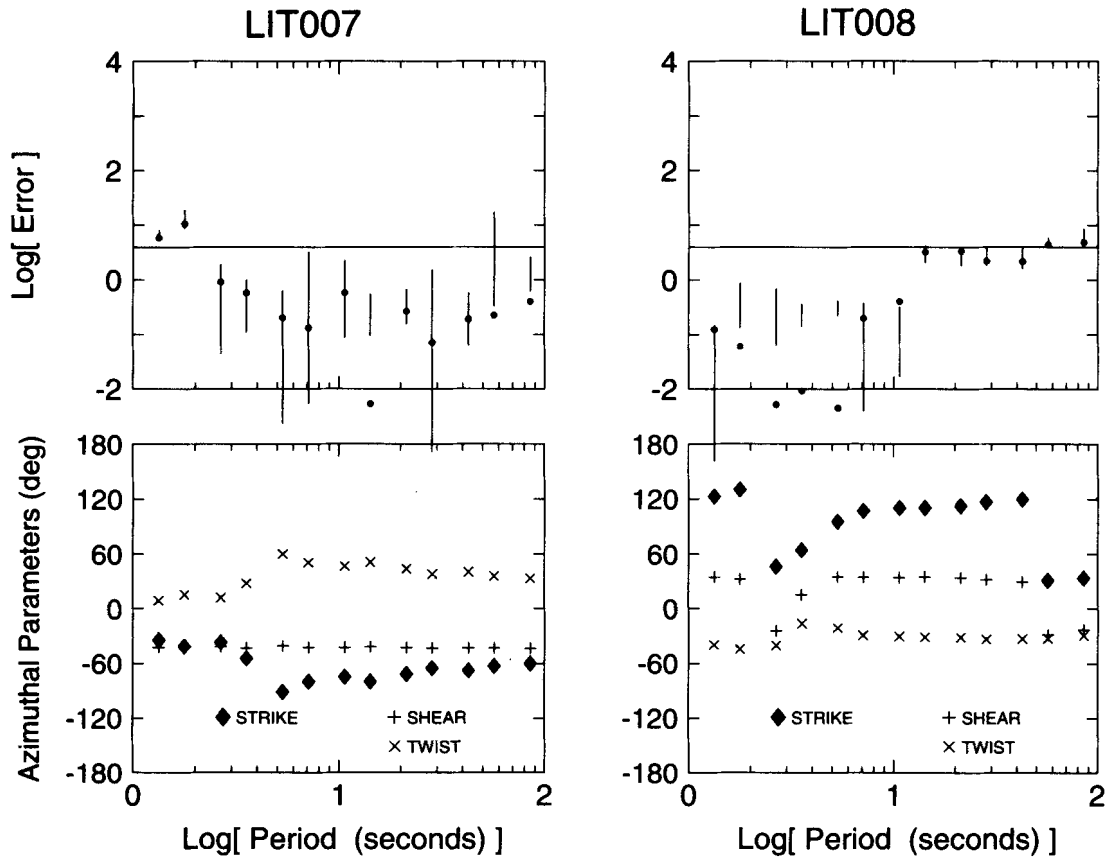

Figure 11. The Groom–Bailey unconstrained distortion parameters for sites *lit007* (left panel) and *lit008* (right panel). The upper diagrams give a χ^2 measure of the misfit error. The symbols are as for Fig. 3.

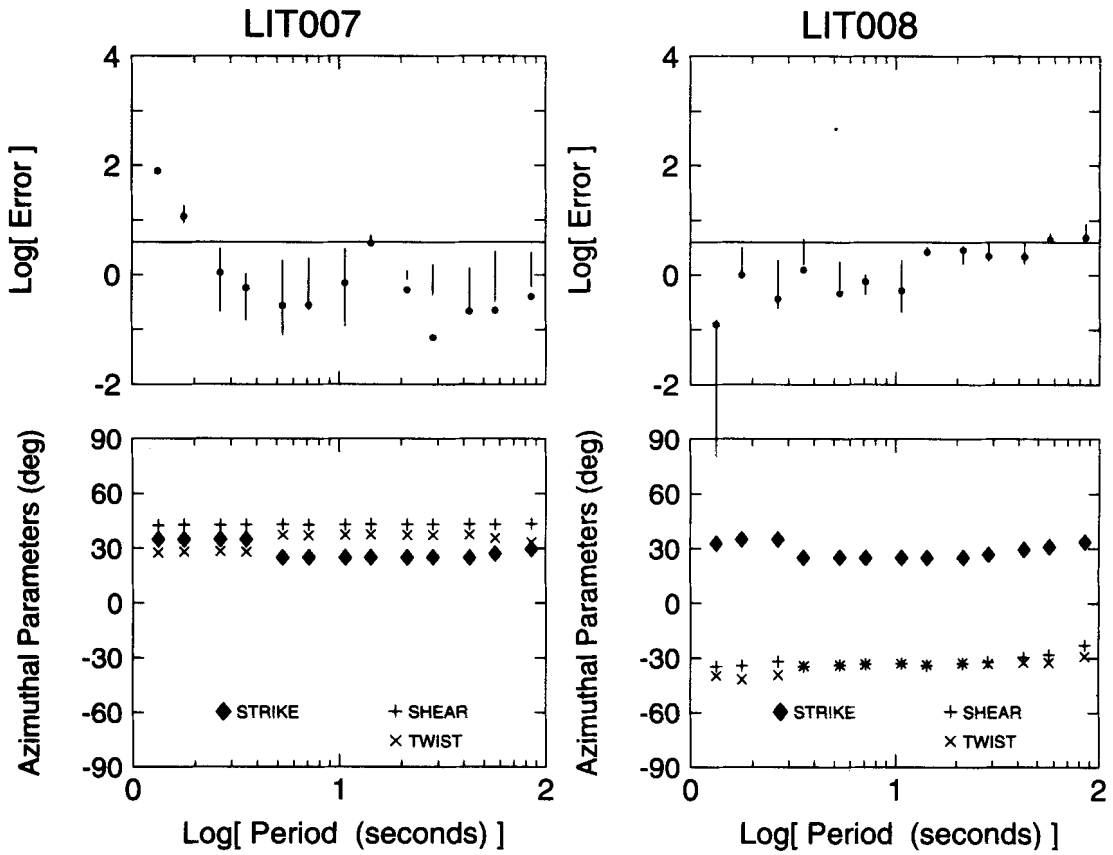

Figure 12. The Groom–Bailey constrained distortion parameters for sites *lit007* (left panel) and *lit008* (right panel) constrained to find strike angles in the range 25° to 35°. The symbols are as for Fig. 3.

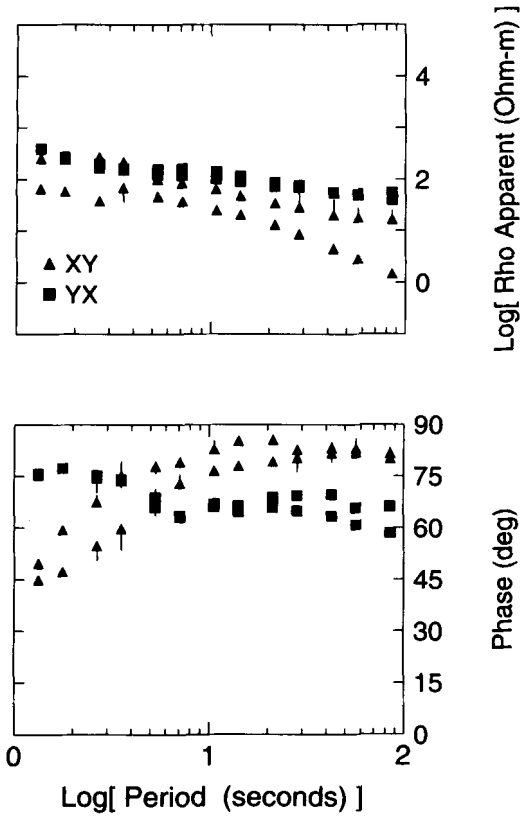

Figure 13. The recovered regional 2-D impedances from *lit007* and *lit008* in the strike coordinate frame of 25° to 35°. The *yx* impedances (*squares*) are particularly well recovered and are virtually identical from both locations.

impedance estimates may vary significantly because of the inherently lower signal-to-noise ratio.

In the case of data from sites at which the local current channelling is very severe, such that the shear (*e*) is unity, the MT data only contain information from a single electric field direction, and no method will ever be able to extract the regional impedances from both modes. MT sites must be located with care to avoid such occurrences; one cannot glibly assume that modern processing methods will compensate for poor field practise.

Finally, although it is beyond the scope of this note to discuss the vertical to horizontal magnetic field transfer functions ('induction arrows'), some workers are using these as an aid to determine the appropriate 2-D strike angle. Whereas this approach may be useful under certain conditions, we caution those who use it that these transfer functions will be affected even more significantly than the MT impedances by the magnetic effects of the galvanic charges as discussed above. Experiments with synthetic data for the embedded hemisphere model of Groom & Bailey (1991), and with other models, indicate that such effects can prohibit the determination of strike direction from the transfer function data alone. This is particularly true for stations in the vicinity of the Nelson batholith (Jones *et al.* 1988), which exhibit systematically distorted induction arrows in the period range 0.1 to 10 s (manuscript in preparation).

ACKNOWLEDGMENTS

During the last four years we have benefited from much fruitful discussion with many of our colleagues, especially Karsten Bahr, David Boerner and Ron Kurtz. Karsten Bahr is particularly thanked for discussions that occurred when one of us (RWG) visited Frankfurt.

The data from the two sites analysed (*lit007* and *lit008*) were acquired as part of the LITHOPROBE program by Phoenix Geophysics (Toronto) Ltd. We thank Phoenix, especially George Elliot and Gerry Graham, for their commitment to high quality data.

Jagdish Gupta and Dave Boerner are acknowledged for their comments on an earlier version of this note, as are Karsten Bahr and the other referee for their thoughtful reviews of the submitted version.

LITHOPROBE Publication No. 333. Geological Survey of Canada Contribution 17292.

REFERENCES

Bahr, K., 1988. Interpretation of the magnetotelluric impedance tensor: regional induction and local telluric distortion, *J. Geophys.*, **62**, 119–127.

Bahr, K., 1991. Geological noise in magnetotelluric data: a classification of distortion types, *Phys. Earth planet. Interiors*, **66**, 24–38.

Chakridi, R., Chouteau, M. & Mareschal, M., 1992. A simple technique for analysing and partly removing galvanic distortion from the magnetotelluric impedance tensor: application to Abitibi and Kapuskasing data (Canada), *Geophys. J. Int.*, **108**, 917–929.

Groom, R. W. & Bahr, K., 1992. Corrections for near surface effects: decomposition of the magnetotelluric impedance tensor and scaling corrections for regional resistivities: A tutorial, *Geophys. Surv.*, **13**, 341–379.

Groom, R. W. & Bailey, R. C., 1989. Decomposition of magnetotelluric impedance tensor in the presence of local three-dimensional galvanic distortion, *J. geophys. Res.*, **94**, 1913–1925.

Groom, R. W. & Bailey, R. C., 1991. Analytical investigations of the effects of near-surface three-dimensional galvanic scatterers on MT tensor decomposition, *Geophysics*, **56**, 496–518.

Groom, R. W., Kurtz, R. D., Jones, A. G. & Boerner, D. E., 1992. A quantitative methodology for determining the dimensionality of conductive structure from magnetotelluric data, *Geophys. J. Int.*, submitted.

Jones, A. G., 1988. Static shift of magnetotelluric data and its removal in a sedimentary basin environment, *Geophysics*, **53**, 967–978.

Jones, A. G. & Craven, J. A., 1990. The North American Central Plains conductivity anomaly and its correlation with gravity, magnetics, seismic, and heat flow data in the Province of Saskatchewan, *Phys. Earth planet. Interiors.*, **60**, 169–194.

Jones, A. G., Kurtz, R. D., Oldenburg, D. W., Boerner, D. E. & Ellis, R., 1988. Magnetotelluric observations along the LITHOPROBE southeastern Canadian Cordilleran transect, *Geophys. Res. Lett.*, **15**, 677–680.

Swift, C. M., 1967. A magnetotelluric investigation of an electrical conductivity anomaly in the south-western United States, *PhD thesis*, Department of Geology and Geophysics, M.I.T., Cambridge, MA.

Zhang, P., Roberts, R. G. & Pedersen, L. B., 1986. Magnetotelluric strike rules, *Geophysics*, **52**, 267–278.